The utility of ^{82}Rb PET for myocardial viability assessment: Comparison with perfusion-metabolism ^{82}Rb-^{18}F-FDG PET

Jonathan B. Moody, PhD,[a] Keri M. Hiller, CNMT, RT(N),[b] Benjamin C. Lee, PhD,[a] Alexis Poitrasson-Rivière, PhD,[a] James R. Corbett, MD,[b,c,d] Richard L. Weinberg, MD,[b,c,d] Venkatesh L. Murthy, MD, PhD,[b,c,d] and Edward P. Ficaro, PhD[a,b,d]

[a] INVIA Medical Imaging Solutions, Ann Arbor, MI
[b] Cardiac Imaging Program, University of Michigan, Ann Arbor, MI
[c] Division of Cardiovascular Medicine, Department of Internal Medicine, University of Michigan, Ann Arbor, MI
[d] Division of Nuclear Medicine, Department of Radiology, University of Michigan, Ann Arbor, MI

Received Mar 20, 2018; accepted May 1, 2018
doi:10.1007/s12350-019-01615-0

Background. **^{82}Rb kinetics may distinguish scar from viable but dysfunctional (hibernating) myocardium. We sought to define the relationship between ^{82}Rb kinetics and myocardial viability compared with conventional ^{82}Rb and ^{18}F-fluorodeoxyglucose (FDG) perfusion-metabolism PET imaging.**

Methods. **Consecutive patients (N=120) referred for evaluation of myocardial viability prior to revascularization and normal volunteers (N=37) were reviewed. Dynamic ^{82}Rb 3D PET data were acquired at rest. ^{18}F-FDG 3D PET data were acquired after metabolic preparation using a standardized hyperinsulinemic-euglycemic clamp. ^{82}Rb kinetic parameters K_1, k_2, and partition coefficient (KP) were estimated by compartmental modeling**

Results. **Segmental ^{82}Rb k_2 and KP differed significantly between scarred and hibernating segments identified by Rb-FDG perfusion-metabolism (k_2, 0.42±0.25 vs. 0.22±0.09 min^{-1}; P <.0001; KP, 1.33±0.62 vs. 2.25±0.98 ml/g; P<.0001). As compared to Rb-FDG analysis, segmental Rb KP had a c-index, sensitivity and specificity of 0.809, 76% and 84%, respectively, for distinguishing hibernating and scarred segments. Segmental k_2 performed similarly, but with lower specificity (75%, P<.001)**

Conclusions. **In this pilot study, ^{82}Rb kinetic parameters k_2 and KP, which are readily estimated using a compartmental model commonly used for myocardial blood flow, reliably differentiated hibernating myocardium and scar. Further study is necessary to evaluate their clinical utility for predicting benefit after revascularization. (J Nucl Cardiol 2019;26:374–86.)**

Spanish Abstract

Antecedentes. **La cinética con ^{82}Rb puede distinguir las cicatrices miocárdicas del tejido viable pero disfuncional (hibernante). Buscamos definir la relación entre la cinética del ^{82}Rb y la**

Electronic supplementary material The online version of this article (https://doi.org/10.1007/s12350-019-01615-0) contains supplementary material, which is available to authorized users.

The authors of this article have provided a Power Point file, available for download at SpringerLink, which summarises the contents of the paper and is free for re-use at meetings and presentations. Search for the article DOI on SpringerLink.com.

Venkatesh L. Murthy and Edward P. Ficaro have contributed equally and also as co-senior authors.

JNC thanks Erick Alexanderson MD, Alondra Flores MD, Jessy Steve Masso MD, and Oscar Perez-Orpinel MD for providing the Spanish abstract; Zhuo He, Haipeng Tang MS, Min Zhao, and Weihua Zhou PhD for providing the Chinese abstract; and Jean-Luc Urbain, MD, PhD, CPE, Past President CANM, Chief Nuclear Medicine, Lebanon VAMC, PA for providing the French abstract.

Reprint requests: Jonathan B. Moody, PhD, INVIA Medical Imaging Solutions, 3025 Boardwalk Street, Suite 200, Ann Arbor, MI 48108; *jmoody@inviasolutions.com*

1071-3581/$34.00

viabilidad miocárdica comparada con las imágenes convencionales de PET con ^{82}Rb y ^{18}F-flurodeoxyglucosa (FDG).

Métodos. **se evaluaron a Pacientes Consecutivos (N=120) referidos para evaluación de viabilidad miocárdica previos a revascularización y voluntarios normales (N=37). Los datos de PET 3D dinámico con ^{82}Rb fueron adquiridos en reposo. Los datos de ^{18}F-FDG 3D PET fueron adquiridos posterior a la preparación metabólica usando un clamp hiperinsulínico-euglucémico. Los patrones cinéticos K1, k2 y el coeficiente de partición (KP) fueron estimados por el modelo compartimental.**

Resultados. **el k2 y KP del ^{82}Rb permitueron distinguier el tejido cicatricial de los segmentos hibernados identificados por la vía perfusión metabolismo de Rb-FDG (k_2, 0.42±0.25 vs. 0.22±0.09 min-1; *P*<.0001; KP, 1.33±0.62 vs. 2.25±0.98 ml/g; *P*<.0001). En comparación con el análisis de Rb-FDG, el KP segmentario del Rb tuvo un índice-c, sensbilidad y especificidad de 0.809 76 y 84%, respectivamente, para distinguir segmentos hibernantes y cicatriciales. k2 Segmentario tuvo un desempeño similar pero con una menor especificidad (75%, *P*<.001).**

Conclusiones. **En este estudio piloto, los parámetros cinéticos k2 y KP del ^{82}Rb, los cuales son estimados usando un modelo compartimental usado comúnmente para flujo sanguíneo miocárdico, diferenciaron el miocardio hibernante del cicatricial. Se necesita estudiar más a fondo para evaluar la utilidad clínica para la predicción del beneficio posterior a la revascularización (J Nucl Cardiol 2019;26:374–86.)**

Chinese Abstract

背景. 铷-82(^{82}Rb)药代动力学可能区分梗死与功能受损但存活的心肌(冬眠心肌)。我们将探讨^{82}Rb药代动力学与存活心肌的关系,并与常规的^{82}Rb和^{18}F-氟脱氧葡萄糖(FDG)灌注-代谢PET显像进行比较。

方法. 连续纳入120名血运重建前评估存活心肌的患者和37名正常志愿者。获得静息^{82}Rb 3D-PET动态采集数据;采用标准化的高胰岛素－正葡萄糖钳夹试验得到^{18}F-FDG 3D PET代谢显像数据; 通过房室模型计算^{82}Rb动力学参数k_1,k_2和分配系数(KP)。

结果. 以Rb-FDG灌注代谢显像鉴定疤痕心肌组和冬眠心肌组,两组的^{82}Rb节段性 k_2值和KP值有明显差异(k_2, 0.42±0.25 vs 0.22±0.09 min^{-1}; *P*<.0001; KP, 1.33±0.62 vs 2.25±0.98 ml/g; *P*<.0001)。以Rb-FDG灌注代谢显像为诊断标准,^{82}Rb节段性 KP对疤痕和冬眠心肌鉴别效能的c指数,敏感性和特异性分别是0.809, 76%和84%。节段性k_2的鉴别效能与KP相似,但特异性较低(75%,*P*<.001)。

结论. 在本试验性研究中,通过常规用于^{82}Rb心肌血流量测定的房室模型计算出的^{82}Rb动力学参数k_2和KP,可以有效的区分冬眠心肌和瘢痕心肌。 但需要进一步的研究来评估其对预测血运重建是否获益的临床价值。 (J Nucl Cardiol 2019;26:374–86.)

French Abstract

Contexte. **La cinétique du ^{82}Rb pourrait être utilisée pour distinguer la fibrose myocardique des zones viables mais dysfonctionnelles (en hibernation). Dans cette étude, nous avons cherché à définir la relation entre la cinétique du ^{82}Rb et la viabilité myocardique en comparant les images de perfusion et métabolisme myocardique utilisant le ^{82}Rb et le ^{18}F-fluorodésoxyglucose (FDG)**

Méthodes. **les données obtenues chez 120 patients consécutifs (N=120) référés pour évaluation de la viabilité du myocarde avant revascularisation et 37 volontaires considérés normaux (N=37) ont été étudieés. Les données TEP 3D dynamiques ^{82}Rb ont été acquises au repos. Les données TEP 3D au ^{18}F-FDG ont été acquises après préparation métabolique utilisant une pince hyperinsulémique-euglycémique normalisée. Les paramètres k1, k2 et le coefficient de partage (KP) de la cinétique du ^{82}R bont été évalues par modélisation compartimentale.**

Résultats. **les paramètres k2 et KP de distribution du ^{82}Rb se sont révélés significativement différent entre les zones tissulaires cicatricielles fibreuses et celles en hibernation identifiées par étude métabolique au FDG (k2, 0,42±0,25 vs. 0,22±0,09 min^{-1}; *P*<0,0001; KP, 1,33±0,62 vs. 2,25±0,98 ml/g; *P*<0,0001). Par rapport aux données FDG, le paramètre KP du rubidium a révélé un indice de concordance de 0,809 et une sensibilité et spécificité de 76% et 84%, pour la distinction des segments en hibernation et cicatrisés. Les résultats du paramètre k2 se sont révélés similaires, mais avec une spécificité plus faible calculée à 75% (*P*<0,001).**

Conclusions. **Dans cette étude pilote, les paramètres cinétiques k2 et KP de perfusion myocardique au ^{82}Rb, qui sont facilement estimés à l'aide d'un modèle compartimental couramment utilisé pour flux sanguin myocardique, ont permis de différencier de manière fiable le myocarde cicatricielle des zones myocardiques hibernantes. Une étude plus approfondie est souhaitable pour valider leur utilité clinique en revacularisation. (J Nucl Cardiol 2019;26:374–86.)**

Key Words: Ischemic cardiomyopathy · cardiac rubidium-82 3D PET · hibernating myocardium · kinetic modeling

Abbreviations	
PET	Positron emission tomography
^{82}Rb	Rubidium-82
^{18}F	Fluorine-18
FDG	Fluorodeoxyglucose
ICM	Ischemic cardiomyopathy
GIR	Glucose infusion rate

See related editorial, pp. 387–390

INTRODUCTION

Non-invasive imaging has long played an essential role in the assessment of myocardial viability.[1] The detection of viable but dysfunctional (hibernating) myocardium has been widely used to predict recovery of contractile function after revascularization.[2,3] Positron emission tomography (PET) with ^{18}F-fluorodeoxyglucose (FDG) is the most sensitive non-invasive test for distinguishing necrotic and hibernating myocardium in patients with severe coronary artery disease and impaired left ventricular function.[2,3] However, FDG PET is expensive, time consuming, and resource intensive. Consequently, it is necessary to target FDG PET viability assessment to those patients where clinical yield is likely to be highest.

Since tissue retention of ^{82}Rb, like ^{201}Tl, provides a measure of the myocardial potassium pool,[4] ^{82}Rb washout was previously studied as an indicator of myocardial cell membrane function.[5,6] ^{82}Rb PET was also compared with FDG PET as a clinical marker of impaired myocardial tissue integrity.[7] Although early results were promising,[8,9] more recent clinical studies [10,11] have been unable to reproduce those results using similar quantitative methods. This discrepancy may be due to subtle but important differences in methodology and/or PET scanner limitations, as well as variations in insulin sensitivity or temporal proximity of myocardial infarction among patient populations, as discussed in detail below.

The use of dynamic 3D PET and compartmental modeling for absolute myocardial blood flow estimation has recently become feasible in routine practice because of improvements in PET scanner performance and clinical software tools.[12] Compartmental modeling of ^{82}Rb PET for myocardial viability assessment has not been previously reported. Our hypothesis is that contemporary PET technology and kinetic modeling may now enable consistent viability assessment with ^{82}Rb imaging alone. The purpose of this study was to re-evaluate the clinical utility of dynamic cardiac ^{82}Rb PET for identification of scar and viable dysfunctional myocardium.

METHODS

Subjects

We retrospectively identified consecutive patients referred between June 2015 and February 2017 to the University of Michigan Cardiovascular Center for viability assessment prior to revascularization, who underwent rest ^{82}Rb and ^{18}F-FDG PET. Informed consent was not required for clinical patients under an exemption from the University of Michigan Institutional Review Board.

An additional group of 37 normal volunteers was included (13 men, 24 women; age 51±11 y; BMI 24.4±2.9 kg/m^2) who were previously prospectively recruited to establish the distribution of ^{82}Rb in normal myocardium. Normal volunteers had no history or clinical symptoms of cardiovascular disease, normal symptom-limited maximal treadmill-exercise electrocardiogram (ECG) test, as well as no perfusion or functional abnormalities on myocardial perfusion ^{82}Rb PET scans. ^{18}F-FDG PET was not performed in these normal volunteers. All normal volunteers provided informed consent under a protocol approved by the University of Michigan Institutional Review Board.

Image Acquisition Protocol

All subjects were instructed to fast for at least 4 hours before the imaging exam. PET/CT imaging was performed in 3D mode on a time-of-flight (TOF) scanner with LSO detectors (Biograph mCT, Siemens, Malvern, PA). An initial CT scan was acquired for attenuation correction. List-mode ECG-gated TOF PET data were acquired for 7 minutes beginning with intravenous bolus injection of ^{82}Rb using a body weight-based dose of 12 MBq/kg (CardioGen-82, Bracco Diagnostics, Monroe Township, NJ). After completion of ^{82}Rb imaging, a hyperinsulinemic-euglycemic clamp was initiated for all patients to establish standardized metabolic conditions for glucose uptake during ^{18}F-FDG PET.[13] In brief, all patients were infused intravenously with 3.33 mU/kg/min of insulin, and capillary (finger-stick) blood glucose was measured every 15 minutes. An intravenous infusion of 20% dextrose was titrated to establish a steady-state blood glucose measurement of 100-140 mg/dl. After at least 60 minutes of

hyperinsulinemia and 30 minutes of steady-state blood glucose conditions, 296-370 MBq of ^{18}F-FDG was injected. Approximately 60 minutes later, list-mode ECG-gated TOF PET data were acquired for 10 minutes followed by a CT scan for attenuation correction. Images were reconstructed and processed as described previously.[14,15]

Rb-FDG Viability Assessment

Perfusion polar maps were generated from static rest ^{82}Rb PET images and normalized to peak ^{82}Rb uptake in the LV. Metabolism polar maps were generated from static FDG PET images and normalized to the FDG uptake at the same myocardial region of peak ^{82}Rb uptake.[16] The standardized uptake value (SUV) of FDG normalized to body weight was also computed.[17] Perfusion polar maps were compared to a matched ^{82}Rb normal database to identify resting perfusion defects (defect threshold was 2.5 SD below normal mean, corresponding to moderate-severe abnormality) [15] which were subsequently used for both Rb-FDG and Rb-only viability analysis. Within the regions of resting perfusion defect, viable (*hibernating*) myocardium was defined by FDG uptake≥50%, and *scar* was defined by FDG uptake<50%.[7,18] A standard 17 segment overlay[19] was applied to each polar map for segmental analysis. Segmental perfusion was automatically scored on a five-point scale from 0-4 (normal, mild, moderate, severe, absent). Segments with perfusion score 1 (mild) were excluded from viability analysis since they were likely to be viable.

Rb-only Viability Assessment

Kinetic modeling of dynamic ^{82}Rb PET data was employed as previously described.[20] Polar maps were generated of fitted kinetic parameters K_1, k_2, and the partition coefficient of ^{82}Rb, KP=K_1/k_2. By definition, KP is equal to the equilibrium concentration of tracer in the myocardium divided by the equilibrium concentration in blood. Within the perfusion defect region, spatially dependent thresholds of K_1, k_2, and KP defining metabolically active (*hibernating*) and inactive (*scar*) myocardium were determined by 10-fold cross validation [21] using Rb-FDG viability polar maps as reference standard. Global and segmental hibernating% and scar% were then calculated as a fraction of the LV for each ^{82}Rb kinetic parameter and %uptake. Since the sum of hibernating% and scar% was equal to the perfusion defect extent%, which was the same for both Rb-only and Rb-FDG analysis, only one of the parameters, hibernating% or scar%, was independently determined: in the results below, scar% is reported. Patients were classified as concordant if the absolute difference in global scar% (Rb-only minus Rb-FDG) was≤10 percentage points.

Insulin Sensitivity Analysis

Hyperinsulinemic-euglycemic clamp data were analyzed to estimate each patient's whole-body insulin sensitivity. During steady-state blood glucose conditions, the average glucose infusion rate (GIR) normalized by body weight was taken as an index of whole-body glucose disposal and insulin sensitivity.[22] Steady-state blood glucose was determined at least 1 hour after the start of insulin infusion and lasting at least 30 minutes with coefficient of variation<10%.

Statistical Analysis

Continuous variables are reported as mean±SD unless noted otherwise. Coefficient of variation was defined as SD/mean. Linear regression and Bland-Altman analysis were used to compare Rb-only and Rb-FDG scar%. Correlations between continuous variables were assessed using Spearman's ρ, and pairwise comparisons using the Mann-Whitney U test with Bonferroni adjustment for multiple comparisons. Univariate logistic regression was used to identify variables that were significantly associated with discordance and thresholds were determined by upper or lower quintiles. Multiple linear regression was used to assess clinical predictors of Rb KP. The McNemar test was employed to compare ROC sensitivities and specificities. Two-sided P values<.05 were considered significant. Statistical analysis was performed using R version 3.2.3 [23] and python version 2.7.5.[24]

RESULTS

Patient Characteristics

A total of 120 consecutive patients referred for PET/CT viability assessment were retrospectively identified. Two patients were excluded: one for missing dynamic Rb PET data and the other because dynamic PET was initiated after radiotracer injection, preventing accurate first-pass quantification. Patient characteristics are shown in Table 1. All patients had moderate to severe LV dysfunction with at least two akinetic segments by gated ^{82}Rb PET. Global left ventricular and ^{82}Rb kinetic parameters derived from PET are shown in Tables 2 and 3.

Global Viability Analysis

Mean LV scar extent by Rb-FDG analysis was 21.0 ±15.5%. Rb-only scar extent from k_2 and KP were not different than Rb-FDG scar (P=.374 and P=.443, respectively), but that from K_1 and % Uptake were significantly lower (P=.0014) (Table 2). Concordance rates were also highest for scar based on KP (85%) and k_2 (78%) (Table 4).

Rb-only (KP) and Rb-FDG LV scar extent were significantly correlated (Figure 1A) (intercept=3.99, slope=0.788, R=0.82, P<.001). In Bland-Altman analysis, the mean difference of global scar was -1.8% (limits of agreement −19.9% to 16.2%) (Figure 1B).

Discordance was not associated with diabetes [odds ratio 0.5, 95% CI (0.2, 1.4), P=.20]. However, discordance was significantly associated with severely reduced

Table 1. Ischemic cardiomyopathy patient characteristics (N = 118)

	N (%)
Male/female	96/22 (81/19)
Age (years)	65±11 (29, 95)[a]
BMI (kg/m^2)	30.0±5.5 (17.8, 42.2)[a]
Obese (BMI≥30 kg/m^2)	54 (46)
Diabetes mellitus	62 (53)
Hypercholesterolemia	82 (69)
Hypertension	82 (69)
History of CABG	42 (36)
History of PCI	53 (45)
History of ICD	40 (34)
History of MI	106 (90)
MI time interval, months	5.0 (0.33, 75.5)[b]
Electrocardiogram	
Normal sinus rhythm	76 (64)
Sinus bradycardia	13 (11)
Electronic pacemaker	20 (17)
LBBB	14 (12)
Atrial fibrillation or flutter	18 (15)
QRS>120 ms	48 (41)
Renal function	
CKD Stage 1	74 (63)
CKD Stage 2-3	33 (28)
CKD Stage 4-5	11 (9)
Medication use	
ACEi/ARB	63 (53)
Beta blocker	95 (81)
Calcium channel blocker	9 (8)
Statin	94 (80)
Diuretic	76 (64)
Digoxin	6 (5)
Insulin and/or metformin	31 (26)

[a]Mean±SD (range)
[b]Median (Interquartile Range) time interval between the most recent MI and ^{18}F-FDG PET
ACEi, angiotensin converting enzyme inhibitor; *ARB*, angiotensin receptor blocker; *BMI*, body mass index; *CABG*, Coronary artery bypass graft; *CKD*, chronic kidney disease; *ICD*, implantable cardioverter defibrillator; *LBBB*, left bundle branch block; *MI*, myocardial infarction; *PCI*, Percutaneous coronary intervention

whole-body glucose disposal (GIR<4.2 mg/kg/min), acute MI within 15 days of FDG PET, and resting heart rate>88 bpm (Table 5). After excluding patients with severe insulin resistance and MI within 15 days, concordance rates for KP and k_2 increased significantly while that of K_1 and % Uptake did not (Table 6).

In multiple linear regression analysis, global Rb KP was independently associated with heart rate (β=0.0324, $P<.0001$), LV ejection fraction (β=0.0392, $P<.0001$), and BMI (β=0.0676, $P=.0001$) ($R=0.563$, $P<.0001$).

A typical concordant patient is shown in Figure 2, and a discordant patient in Figure 3; additional cases are shown in Supplemental Figures. 1-5.

Insulin Sensitivity

Median [IQR] GIR was 5.01 (4.45, 6.58). Diabetic patients had significantly lower GIR compared to non-diabetics [4.94 (4.07, 5.70) vs 5.59 (4.96, 6.83), $P<.001$]. Patients in the lowest quintile of GIR (< 4.2 mg/kg/min) had significantly lower FDG SUV myocardium-to-blood ratio in segments with normal perfusion and wall motion at rest [17.6 (6.9, 23.1) vs 23.7 (18.2, 36.1), $P<.001$] (Supplemental Figures. 10-11).

Segmental Viability Analysis

A total of 2,635 segments were analyzed (629 in normal volunteers, 2,006 in patients). In patients, 1024 segments (51%) were normally perfused at rest (perfusion score=0), of which 584 (57%) had abnormal wall motion. 692 abnormally perfused segments (34%) had perfusion score≥2 at rest, and of these, 305 (44%) were classified as hibernating and 387 (56%) as scar by Rb-FDG PET (the remaining 290 segments were mildly abnormal (perfusion score 1) and were excluded from viability analysis). In Figure 4, median segmental ^{82}Rb K_1, k_2, and KP are shown in normally perfused segments at rest in normal volunteers and patients, and in abnormal segments classified as hibernating or scar by Rb-FDG PET. K_1 was not significantly different between normal segments of volunteers and patients, nor between hibernating and scarred segments in patients. All other pairwise differences were significant ($P<.0001$). Segmental KP was significantly correlated with Rb %Uptake and FDG %Uptake (both $P<.0001$, Supplemental Figures. 6-7). Segmental ROC analysis results for all patients are shown in Table 7, and in patients without severe insulin resistance or recent MI in Table 8. Among the Rb kinetic parameters, KP had the highest overall performance for detecting hibernating segments in terms of Youden index (true positive fraction minus false positive fraction).

DISCUSSION

Myocardial ^{82}Rb kinetics were quantified in this study in terms of uptake and washout rates (K_1 and k_2), and the ^{82}Rb partition coefficient (also called *distribution volume*), defined as $KP = K_1/k_2$. Compared to perfusion-metabolism Rb-FDG PET, our results showed

Table 2. Global left ventricular PET imaging parameters (N = 118 patients)

PET imaging parameter	Mean ± SD (range)
Presence and severity of disease	
Summed rest score	21 ± 9 (4, 45)
Rest perfusion defect extent (%)	40.5 ± 15.3 (8.3, 73.5)
LV ejection fraction (%)[a]	32 ± 12 (9, 70)
LV dyssynchrony (%)[a,b]	18 ± 5 (5, 31)
Viability assessment	
Rb-FDG scar extent (%)	21.0 ± 15.5 (0.0, 57.6)
Rb-Only scar extent from KP (%)	20.5 ± 14.8 (0.0, 57.8)
Rb-Only scar extent from k_2 (%)	19.6 ± 13.2 (0.2, 54.6)
Rb-Only scar extent from K_1 (%)	14.4 ± 10.2 (0.0, 41.1)*
Rb-Only scar extent from %Uptake (%)	15.6 ± 13.4 (0.0, 57.0)*

LV, left ventricular; *IQR*, interquartile range; *KP*, ^{82}Rb partition coefficient
*P < .01 compared to Rb-FDG scar extent
[a]Estimated from ECG-gated ^{82}Rb PET
[b]Phase standard deviation of time-to-peak thickening as a percentage of RR cycle[36]

Table 3. Global left ventricular ^{82}Rb PET kinetic parameters [Median (IQR)]

^{82}Rb PET kinetic parameter	ICM patients (N = 118)	Normal volunteers (N = 37)
KP[†]	2.87 (2.28, 3.70)	2.99 (2.59, 3.36)
k_2	0.24 (0.18, 0.30)	0.21 (0.19, 0.24)*
K_1	0.54 (0.49, 0.59)	0.57 (0.54, 0.64)**

ICM, ischemic cardiomyopathy; *IQR*, interquartile range
*P < .05
**P < .01 (Mann-Whitney U test)
[†]Partition coefficient of ^{82}Rb defined as K_1/k_2

Table 4. Concordance between Rb-FDG and Rb-only viability assessment (N = 118 patients). Rb-only LV scar% was estimated by each of the ^{82}Rb parameters and compared with Rb-FDG LV scar%. Concordant patients were defined as those having absolute scar difference < 10%

^{82}Rb PET kinetic parameter	Concordance rate (%) (N)	95% CI (%)
KP	85 (100)	(78, 91)
k_2	78 (92)	(70, 85)
K_1	63 (74)*	(54, 71)
% Uptake	74 (87)	(66, 82)

N, number of patients; *CI*, confidence interval
*P < .05 compared to Rb KP

that both KP and k_2 accurately differentiated metabolically active (hibernating) myocardium and scar in patients with chronic ischemic cardiomyopathy (Table 4 and Table 6). On a segmental basis, both KP and k_2 were significantly different between hibernating and scarred segments (Figure 4), and both parameters had similar

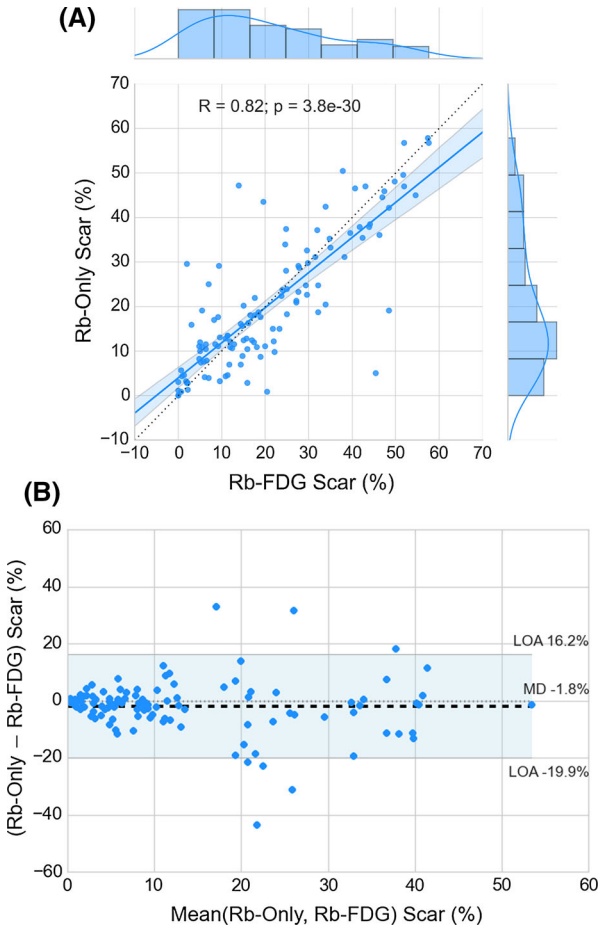

Figure 1. **A** Linear correlation of global extent of LV scar (%) estimated from Rb-only (KP) and perfusion-metabolism Rb-FDG PET. Dotted line is the line of identity and solid line is the fitted linear regression. **B** Bland-Altman plot. Shaded regions are 95% confidence intervals of the regression estimate (**A**) and 95% limits of agreement (**B**) (N=118 patients). (*MD*, mean difference; *LOA*, limits of agreement).

sensitivity for detecting hibernating segments, although KP had somewhat higher specificity (Table 7 and Table 8). These results are consistent with the known behavior of ^{82}Rb as a potassium analog in the heart [5,6] and prior clinical studies of ^{82}Rb myocardial washout.[7–9] They also suggest the feasibility of greatly simplifying the standard Rb-FDG PET viability protocol by omitting the necessary glucose metabolic preparation and FDG PET scan, as well as reducing radiation dose to the patient.

Concordance of Rb-FDG and Rb-only Viability

Concordance between Rb-FDG and Rb-only KP was observed in 85% (100/118, Table 4) of patients in this study. In close review of the discordant patients, it was found that these patients were more likely to exhibit severely reduced whole-body insulin sensitivity, to have myocardial infarction within 15 days of FDG PET, or to have high resting heart rate (Table 5). Myocardial insulin resistance has been previously reported in patients with ischemic cardiomyopathy and whole-body insulin resistance.[25] The association with low insulin sensitivity raises the possibility that in some patients a reduced myocardial glucose uptake may have confounded the comparison with viability based on Rb kinetics. Further, FDG uptake in patients with recent MI may have been elevated by regional myocardial inflammation. Importantly, after excluding patients with either of these potentially confounding factors, the concordance rates for both Rb KP and k_2 increased markedly to 96% (65/68) and 85% (58/68), respectively. Likewise, the sensitivity and specificity for detecting hibernating segments increased for Rb KP and k_2 (Table 8).

Table 5. Univariate associations of discordance between Rb-FDG and Rb-only viability (cut-offs were determined by lowest or highest quintiles)

Clinical variable	Odds ratio	95% CI	*P* value
Severe insulin resistance, GIR<4.2 mg/kg/min	3.6	(1.3, 10.5)	0.017
Myocardial infarction within 15 days of ^{18}F-FDG PET	5.3	(1.8, 15.1)	0.002
Resting heart rate>88 bpm	4.2	(1.4, 12.3)	0.009

GIR, glucose infusion rate; CI, confidence interval

Table 6. Concordance between Rb-FDG and Rb-only viability assessment after excluding patients with severe insulin resistance (GIR<4.2 mg/kg/min) and MI within 15 days of FDG PET (N=68 patients)

^{82}Rb PET kinetic parameter	Concordance rate (%) (N)	95% CI (%)
KP	96 (65)	(91, 100)
k_2	85 (58)	(77, 94)
K_1	62 (42)*	(50, 73)
% Uptake	76 (52)*	(66, 87)

N, number of patients; *CI*, confidence interval
*P<.05 compared to Rb KP

^{82}Rb Kinetic Model

The same kinetic model (one-tissue compartment, 1TC) that has been widely implemented for clinical myocardial blood flow estimation via K_1 [26] was employed in this study to estimate ^{82}Rb kinetic parameters. The model parameter, k_2, representing tracer washout rate, has typically been treated as a nuisance parameter and either fixed to a constant global value in the model [27] or simply discarded after fitting the model. The present study demonstrates the utility of retaining k_2 to more fully utilize the clinically relevant information available in the dynamic PET data.

vom Dahl et al. [9] suggested that viability assessment using myocardial ^{82}Rb kinetics may be best approached using the ^{82}Rb partition coefficient, KP, although technical limitations at that time prevented its use. KP reflects the equilibrium partition of ^{82}Rb between myocardium and blood, and values greater than 1 indicate active cellular transport and metabolism. Although equilibrium will not, in general, be reached after bolus tracer injection during the 7-minute ^{82}Rb PET scan, the relationship between KP and the rate parameters K_1 and k_2 allows the partition coefficient to be estimated without directly observing the equilibrium condition.

Alternative Methods

Prior studies [7–9] focused on estimating ^{82}Rb washout rates using either the ratio of late-to-early myocardial activity [7,8] or by fitting a decaying mono-exponential model to myocardial time-activity curves (TACs) after tracer clearance from blood.[9] These heuristic methods were used for ease of use in the clinical setting [7,8] or due to PET scanner limitations for dynamic ^{82}Rb image acquisition.[9] Two more recent clinical studies [10,11] used similar methods but failed to distinguish hibernating and infarcted myocardium using ^{82}Rb washout alone. Several factors may have contributed to these previous inconsistent results.

First, it has been previously demonstrated [28] that tracer recirculation can affect mono-exponential washout estimation in two ways: the fitted decay constants will underestimate the true washout rate, and variability of these decay constants will be increased (although this was demonstrated for ^{11}C-acetate, the effects are quite general and apply to any tracer which is partially extracted after bolus intravenous injection). The flow-dependent myocardial extraction fraction of ^{82}Rb has been reported to be in the range 0.4 to 0.7 at resting flows,[29–32] thus a substantial fraction of the tracer will recirculate. Patient-specific variations in the amount of recirculating tracer will produce variations in the LV arterial input function. We verified using simulation methods similar to Buck et al.[28] that these same effects occur for clinical ^{82}Rb input functions (Supplemental Figure 12). Second, washout based on late-to-early image ratios, with [7] or without [10] constant background subtraction, may have similar additional variability because such ratios do not account for the effects of tracer recirculation. In contrast, the ^{82}Rb 1TC kinetic model does account for recirculating tracer by explicit deconvolution of the arterial input function.[28] Third, the extremely short half-life of ^{82}Rb (76 s) limits the sensitivity of image ratios to detect mild to moderate increases in washout. Fourth, variations in the approach to normalizing FDG uptake can adversely affect the viability reference standard [10,11,16,33]

Advantages and Added Value of ^{82}Rb Kinetics

Viability assessment using ^{82}Rb kinetics has several advantages compared to Rb-FDG, including the ability to assess perfusion and metabolism with one radiopharmaceutical injection; a much shorter PET imaging protocol without the need for exogenous metabolic standardization; potentially improved reliability in patients with insulin resistance and diabetes; and perfect spatial registration of image data used to assess

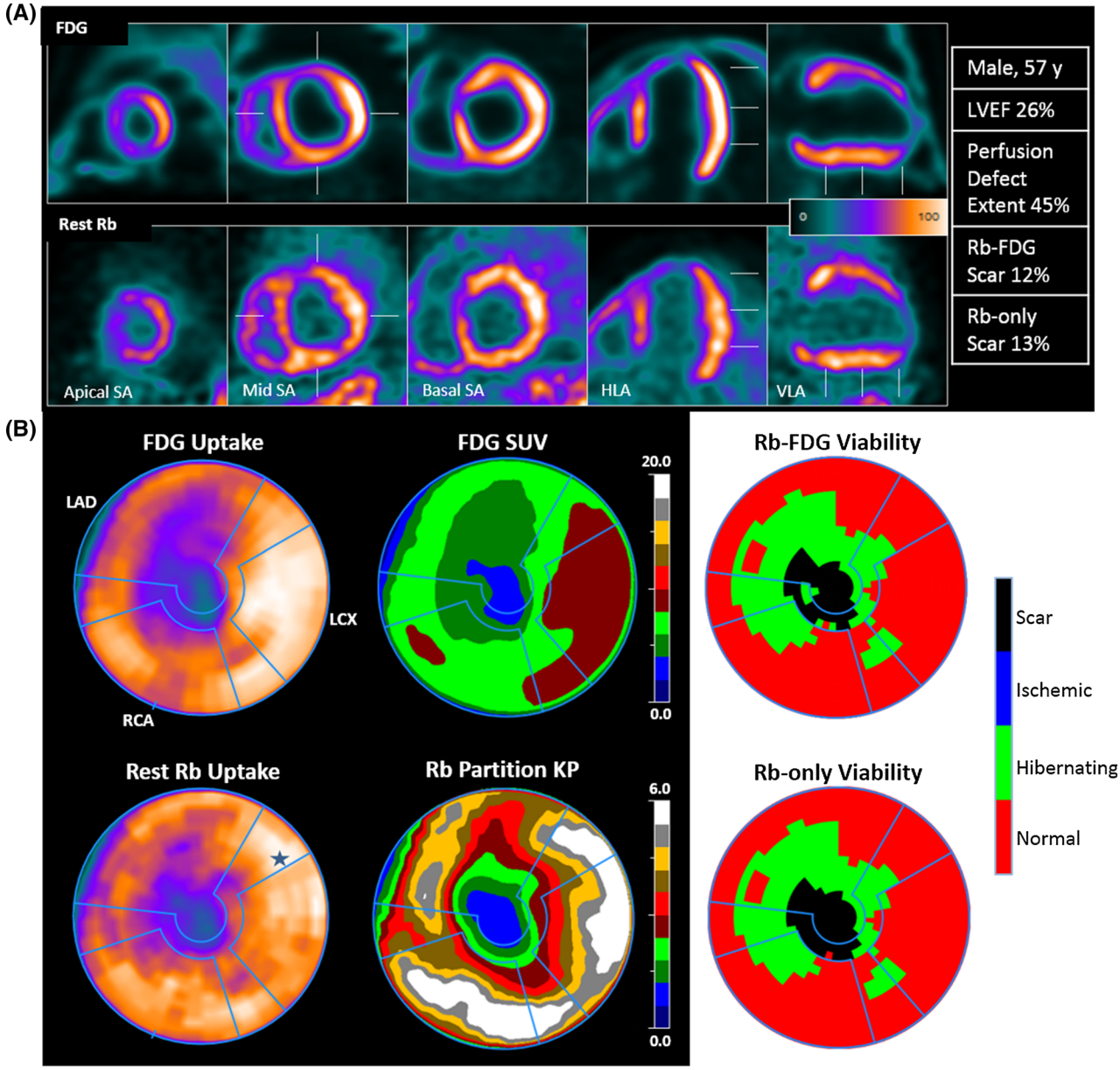

Figure 2. A concordant case without diabetes (glucose infusion rate, GIR 8.8 mg/kg/min) and predominant hibernating myocardium. **A** Images showed a large-sized, moderate to severe apical, anterior, anteroseptal, and inferoseptal resting perfusion defect (total extent 45%). **B** Polar maps: the global Rb-FDG scar was 12% of the LV and Rb-only (KP) scar was 13%. Images and uptake polar maps use a common color scale (0-100%). The star on the Rest Rb Uptake polar map indicates the region used for uptake normalization. Vascular territories: *LAD*, left anterior descending; *LCX*, left circumflex; *RCA*, right coronary artery, *SUV*, standardized uptake value.

perfusion and metabolism. The shorter imaging protocol would also facilitate easier evaluation of inducible ischemia by the addition of pharmacologic stress to the ^{82}Rb PET protocol.

^{82}Rb %uptake was significantly correlated with KP (Supplemental Figure 7) and Rb-only viability assessment by %uptake performed reasonably well. In the overall study group, ^{82}Rb %uptake provided patient-

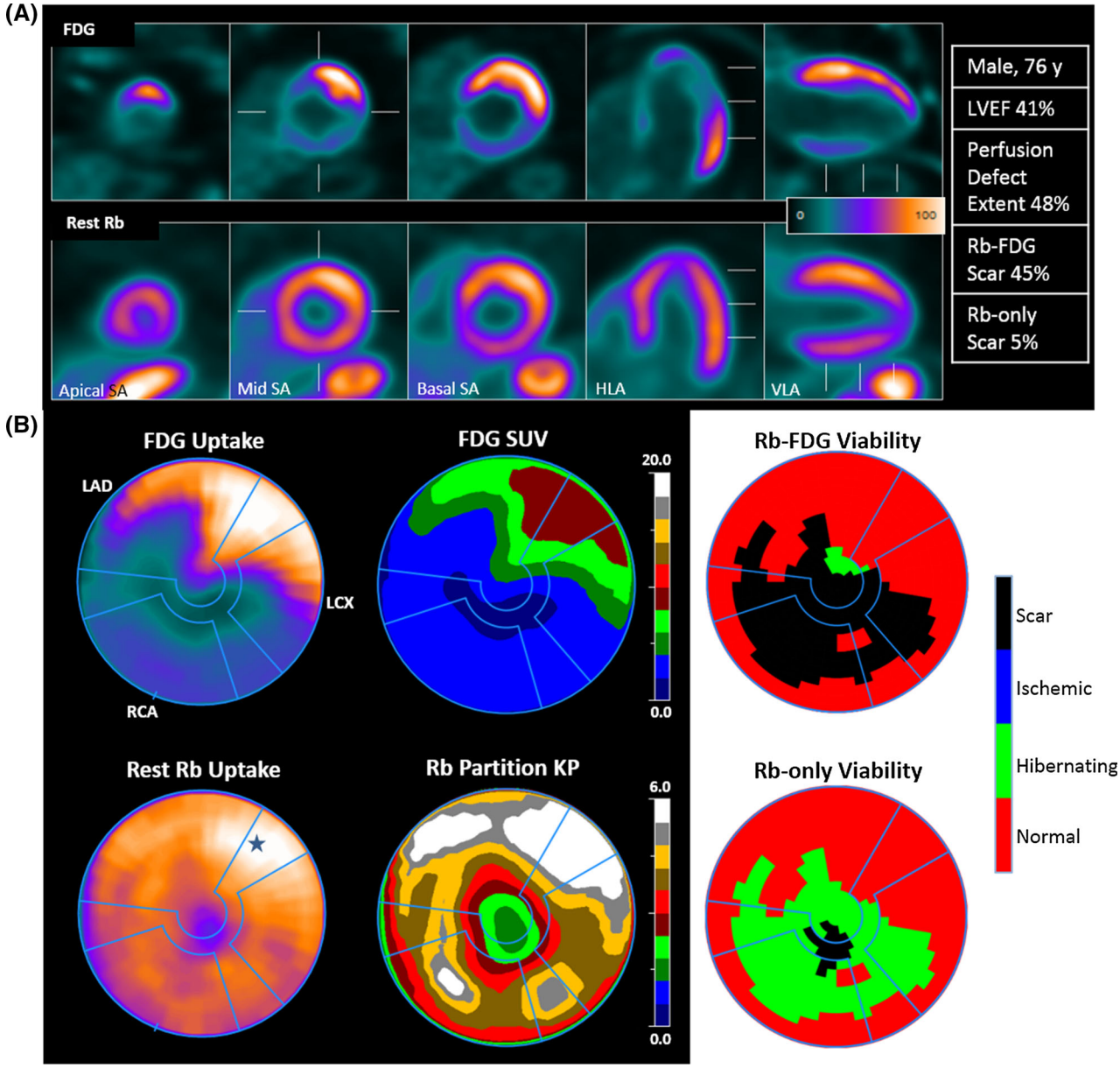

Figure 3. A discordant case with paroxysmal atrial fibrillation and severely reduced whole-body insulin sensitivity (glucose infusion rate, GIR 3.34 mg/kg/min). **A** Images showed mild to moderate rest defects in apical, septal, inferolateral, lateral, inferoseptal, and inferior regions (total extent 48%). **B** Polar maps: the Rb-FDG global scar was 45% of the LV and Rb-only (KP) scar was 5%. Images and uptake polar maps use a common color scale (0-100%). The star on the Rest Rb Uptake polar map indicates region used for uptake normalization. Vascular territories: *LAD*, left anterior descending; *LCX*, left circumflex; *RCA*, right coronary artery; *SUV*, standardized uptake value.

level concordance that was not statistically different from KP and k_2 (Table 4), as well as the highest sensitivity at the segmental level (although specificity, PPV, and Youden index were inferior to KP, Table 7). These results suggest the possibility that kinetic modeling may not be necessary for viability assessment. However, after excluding patients with severe insulin resistance or recent MI, ^{82}Rb KP improved markedly and was clearly superior to %uptake, both in patient-level concordance (Table 6) as well as in detecting

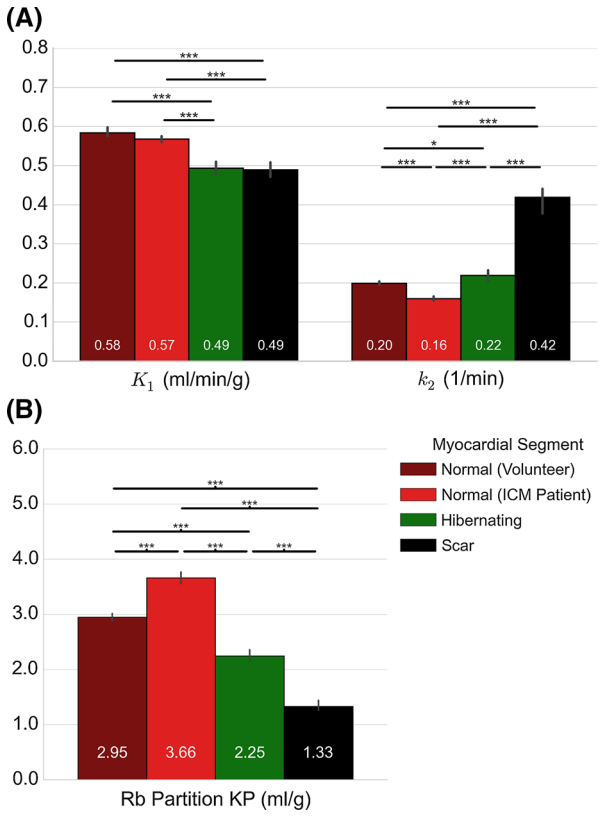

Figure 4. Segmental ^{82}Rb kinetic parameters. **A** Myocardial uptake rate K_1 (ml/min/g), washout rate k_2 (1/min), and **B** Rb partition coefficient KP determined by dynamic 3D PET in LV myocardial segments normally perfused at rest and in segments classified as hibernating or scar by Rb-FDG PET (median ± 95% confidence interval). *ICM*, ischemic cardiomyopathy. (*P<.05, ***P<.0001, Mann-Whitney U test).

hibernating segments (Table 8). The added value of KP for viability assessment may be similar to the added value of absolute myocardial blood flow for CAD assessment, namely, to provide robustness against potential normalization errors that frequently occur for %uptake in cases with multivessel or balanced disease.

Study Limitations

There were several limitations in our study. First, the retrospective nature of this study prevented a characterization of the presence of myocardial ischemia or stunning since the majority of patients did not undergo stress ^{82}Rb PET. Second, an important limitation of substituting FDG PET metabolic assessment with Rb-only KP is the lower spatial resolution of Rb relative to FDG PET [34] which may adversely affect the ability of Rb images to identify small non-transmural scar. Third, although the kinetic parameter thresholds for hibernating myocardium and scar were determined using robust statistical methods, generalizing these thresholds to larger patient populations, and with different PET/CT scanners and acquisition protocols will require further study.

CONCLUSION

Current-generation 3D PET/CT systems are capable of reliable dynamic cardiac PET [35] and clinical kinetic modeling.[26] The ^{82}Rb partition coefficient, KP, an index of the myocardial potassium pool, is readily estimated using the same protocol and kinetic model commonly used for myocardial blood flow, and can be

Table 7. Segmental ROC detection of hibernating myocardial segments using ^{82}Rb kinetic parameters relative to Rb-FDG PET (N = 692 segments, 118 patients)

^{82}Rb PET kinetic parameter	Sensitivity (%)	Specificity (%)	PPV (%)	NPV (%)	c-Index	Youden index
KP	76	84†	80‡	85	0.809	0.599‡
k_2	77	75	72	83	0.803	0.525
K_1	76	43*	52*	75	0.498*	0.195*
% Uptake	88**	63	66	88	0.839	0.509

K_1 units = ml/min/g; k_2 units = min^{-1}; KP = partition coefficient of ^{82}Rb
*P<.001 compared to KP and k_2
**P<.05 compared to KP and K_1 and k_2
†P<.001 compared to K_1 and k_2 and % Uptake
‡P<.05 compared to K_1 and % Uptake

Table 8. Segmental ROC analysis as in Table 7 for the subset of patients without severe insulin resistance (GIR<4.2 mg/kg/min) or MI within 15 days of FDG PET (N = 376 segments, 68 patients)

^{82}Rb PET Kinetic parameter	Sensitivity (%)	Specificity (%)	PPV (%)	NPV (%)	c-Index	Youden index
KP	84	89	84	89	0.831	0.735
k_2	84	82	76	88	0.851	0.653
K_1	82	44*	50*	78	0.469*	0.264*
% Uptake	89	68‡	67†	89	0.856	0.571‡

K_1 units = ml/min/g; k_2 units = min^{-1}; KP = partition coefficient of ^{82}Rb
*P<.001 compared to KP and k_2
†P<.05 compared to KP
‡P<.05 compared to KP and k_2

obtained at no additional cost, imaging time, or radiation exposure. Our results confirm the feasibility of using ^{82}Rb kinetics to differentiate scar and hibernating myocardium. However, further study is necessary to delineate its clinical utility for predicting benefit after revascularization.

NEW KNOWLEDGE GAINED

To our knowledge, this is the first study to apply dynamic ^{82}Rb 3D PET and state-of-the-art compartmental modeling for clinical viability testing, with the evaluation of multiple ^{82}Rb kinetic parameters. Our results suggest that the partition coefficient, KP, is the most suitable ^{82}Rb parameter for distinguishing scar and viable dysfunctional myocardium.[9]

Acknowledgements

The authors thank Erin Pollock and Amanda Melvin for assistance with data collection.

Disclosure

J.B. Moody, B.C. Lee, and A. Poitrasson-Rivière are employees of INVIA. K.M. Hiller has nothing to declare. R.L. Weinberg has nothing to declare. E.P. Ficaro and J.R. Corbett are stockholders of INVIA, which produces 4DM, a clinical software package for cardiac PET analysis. V.L. Murthy declares research support from INVIA, LLC, and stock interest in General Electric, Mallinckrodt, Cardinal Health.

References

1. Anavekar NS, Chareonthaitawee P, Narula J, Gersh BJ. Revascularization in patients with severe left ventricular dysfunction: is the assessment of viability still viable? J Am Coll Cardiol 2016;67(24):2874-87.
2. Schinkel AFL, Bax JJ, Poldermans D, Elhendy A, Ferrari R, Rahimtoola SH. Hibernating myocardium: diagnosis and patient outcomes. Curr Probl Cardiol 2007;32(7):375-410.
3. Allman KC. Noninvasive assessment myocardial viability: Current status and future directions. J Nucl Cardiol 2013;20(4):618-37.
4. Schelbert HR. Positron emission tomography of the heart: Methodology, findings in the normal and the diseased heart, and clinical applications. In: Phelps ME, editor. PET: Molecular Imaging and Its Biological Applications. 1st ed. New York: Springer-Verlag; 2004. p. 389-508.
5. Goldstein RA. Kinetics of rubidium-82 after coronary occlusion and reperfusion. Assessment of patency and viability in open-chested dogs. J Clin Invest 1985;75(4):1131-1137.
6. Goldstein RA. Rubidium-82 kinetics after coronary occlusion: temporal relation of net myocardial accumulation and viability in open-chested dogs. J Nucl Med 1986;27(9):1456-61.
7. Gould KL, Yoshida K, Hess MJ, Haynie M, Mullani N, Smalling RW. Myocardial metabolism of fluorodeoxyglucose compared to cell membrane integrity for the potassium analogue rubidium-82 for assessing infarct size in man by PET. J Nucl Med 1991;32(1):1-9.
8. Yoshida K, Gould KL. Quantitative relation of myocardial infarct size and myocardial viability by positron emission tomography to left ventricular ejection fraction and 3-year mortality with and without revascularization. J Am Coll Cardiol 1993;22(4):984-97.
9. vom Dahl J, Muzik O, Wolfe ER, Allman C, Hutchins G, Schwaiger M. Myocardial rubidium-82 tissue kinetics assessed by dynamic positron emission tomography as a marker of myocardial cell membrane integrity and viability. Circulation 1996;93(2):238-45.
10. Stankewicz MA, Mansour CS, Eisner RL, et al. Myocardial viability assessment by PET: ^{82}Rb defect washout does not predict the results of metabolic-perfusion mismatch. J Nucl Med 2005;46(10):1602-9.
11. Chien DT, Bravo P, Higuchi T, Merrill J, Bengel FM. Washout of ^{82}Rb as a marker of impaired tissue integrity, obtained by list-mode cardiac PET/CT: relationship with perfusion/metabolism patterns of myocardial viability. Eur J Nucl Med Mol Imaging 2011;38(8):1507-15.
12. Moody JB, Lee BC, Corbett JR, Ficaro EP, Murthy VL. Precision and accuracy of clinical quantification of myocardial blood flow by dynamic PET: A technical perspective. J. Nucl. Cardiol 2015;22(5):935-51.

13. Knuuti MJ, Nuutila P, Ruotsalainen U, et al. Euglycemic hyperinsulinemic clamp and oral glucose load in stimulating myocardial glucose utilization during positron emission tomography. J Nucl Med 1992;33(7):1255-62.
14. Lee BC, Moody JB, Poitrasson-Rivière A, et al. Blood pool and tissue phase patient motion effects on ^{82}rubidium PET myocardial blood flow quantification. J Nucl Cardiol 2018;23:1-12.
15. Ficaro EP, Lee BC, Kritzman JN, Corbett JR. Corridor4DM: the Michigan method for quantitative nuclear cardiology. J Nucl Cardiol 2007;14(4):455-65.
16. Porenta G, Kuhle W, Czernin J, et al. Semiquantitative assessment of myocardial blood flow and viability using polar map displays of cardiac PET images. J Nucl Med 1992;33(9):1628-36.
17. FDG-PET/CT Technical Committee. FDG-PET/CT as an Imaging Biomarker Measuring Response to Cancer Therapy. Quantitative Imaging Biomarker Alliance, Version 1.05, Publicly Reviewed Version. QIBA; 2013. https://rsna.org/qiba. Accessed Feb 17, 2016.
18. Knuuti J, Schelbert HR, Bax JJ. The need for standardisation of cardiac FDG PET imaging in the evaluation of myocardial viability in patients with chronic ischaemic left ventricular dysfunction. Eur J Nucl Med Mol Imaging 2002;29(9):1257-66.
19. Cerqueira MD, Weissman NJ, Dilsizian V, et al. Standardized myocardial segmentation and nomenclature for tomographic imaging of the heart. A statement for healthcare professionals from the cardiac imaging committee of the council on clinical cardiology of the American Heart Association. Circulation 2002;105(4):539-42.
20. Moody JB, Murthy VL, Lee BC, Corbett JR, Ficaro EP. Variance estimation for myocardial blood flow by dynamic PET. IEEE Trans Med Imaging 2015;34(11):2343-53.
21. Hastie T, Tibshirani R, Friedman J. The elements of statistical learning: data mining, inference, and prediction. 2nd ed. New York: Springer; 2009.
22. Muniyappa R, Lee S, Chen H, Quon MJ. Current approaches for assessing insulin sensitivity and resistance in vivo: advantages, limitations, and appropriate usage. Am J Physiol 2008;294(1):E15-26.
23. R Core Team. R: a language and environment for statistical computing. Vienna, Austria: R Foundation for Statistical Computing; 2012. http://www.R-project.org/.
24. Millman KJ, Aivazis M. Python for scientists and engineers. Comput Sci Eng 2011;13(2):9-12.
25. Paternostro G, Camici PG, Lammertsma AA, et al. Cardiac and skeletal muscle insulin resistance in patients with coronary heart disease. A study with positron emission tomography. J Clin Invest 1996;98(9):2094-9.
26. Nesterov SV, Deshayes E, Sciagrà R, et al. Quantification of myocardial blood flow in absolute terms using ^{82}Rb PET imaging: results of RUBY-10 study. JACC Cardiovasc Imaging 2014;7(11):1119-27.
27. Klein R, Renaud JM, Ziadi MC, et al. Intra- and inter-operator repeatability of myocardial blood flow and myocardial flow reserve measurements using rubidium-82 PET and a highly automated analysis program. J Nucl Cardiol 2010;17:600-16.
28. Buck A, Wolpers HG, Hutchins GD, et al. Effect of carbon-11-acetate recirculation on estimates of myocardial oxygen consumption by PET. J Nucl Med 1991;32(10):1950-7.
29. Budinger TF, Yano Y, Huesman RH, et al. Positron emission tomography of the heart. Physiologist 1983;26(1):31-4.
30. Mullani NA, Goldstein RA, Gould KL, et al. Myocardial perfusion with rubidium-82. I. Measurement of extraction fraction and flow with external detectors. J Nucl Med 1983;24(10):898-906.
31. Lortie M, Beanlands RSB, Yoshinaga K, Klein R, Dasilva JN, DeKemp RA. Quantification of myocardial blood flow with ^{82}Rb dynamic PET imaging. Eur J Nucl Med Mol Imaging 2007;34(11):1765-74.
32. Prior JO, Allenbach G, Valenta I, et al. Quantification of myocardial blood flow with ^{82}Rb positron emission tomography: clinical validation with ^{15}O-water. Eur J Nucl Med Mol Imaging 2012;39(6):1037-47.
33. Schwaiger M, Pirich C. Reverse flow-metabolism mismatch: what does it mean? J Nucl Med 1999;40(9):1499-502.
34. Johnson NP, Sdringola S, Gould KL. Partial volume correction incorporating Rb-82 positron range for quantitative myocardial perfusion PET based on systolic-diastolic activity ratios and phantom measurements. J Nucl Cardiol 2011;18(2):247-58.
35. Renaud JM, Yip K, Guimond J, et al. Characterization of 3D PET systems for accurate quantification of myocardial blood flow. J Nucl Med 2017;58(1):103-9.
36. AlJaroudi W, Jaber WA, Grimm RA, Marwick T, Cerqueira MD. Alternative methods for the assessment of mechanical dyssynchrony using phase analysis of gated single photon emission computed tomography myocardial perfusion imaging. Int J Cardiovasc Imaging 2012;28(6):1385-94.